Journal of Alloys and Compounds 484 (2009) 86–89

Contents lists available at ScienceDirect

Journal of Alloys and Compounds

journal homepage: www.elsevier.com/locate/jallcom

Phase relations in the Cu-poor part of the Ce–Al–Cu system at 503 K

Q.R. Yao[a,*], X.D. Hu[a,b], X.J. Chen[a], S.K. Pan[a], W. Zou[c], H.L. Wang[a], Y.C. Wang[b], P.P. Wang[a], F. Liu[a], Z.M. Wang[a], H.Y. Zhou[a], C.Y. Tang[a]

[a] Department of Information Materials Science and Engineering, Guilin University of Electronic Technology, Guangxi 541004, PR China
[b] Beijing National Laboratory for Condensed Matter Physics, Institute of Physics, Chinese Academy of Sciences, Beijing 100190, PR China
[c] School of Application Science, Jiangxi University of Science and Technology, Ganzhou, Jiangxi 341000, China

ARTICLE INFO

Article history:
Received 29 November 2008
Received in revised form 22 March 2009
Accepted 23 March 2009
Available online 31 March 2009

Keywords:
Ce–Al–Cu system
Rare earth compounds
Phase relations
Crystal structure
X-ray diffraction

ABSTRACT

The phase relations of the ternary system Ce–Al–Cu in the Cu-poor part at 503 K were investigated by X-ray powder diffraction (XRD). The investigated composition region consists of 16 single-phase, 32 two-phase and 17 three-phase regions. At 503 K, the maximum solid solubilities of Cu in Al, α-Ce_3Al_{11}, $CeAl_3$ and $CeAl_2$ are about 2.5 at.%, 1.6, 3.6 and 5.3, respectively, and Al in $CeCu_5$ is about 39.2 at.%. The homogeneity ranges of Al_2Cu and AlCu phases extend from about 32.1 to 32.6 at.% Cu and 49.7 to 52.4 at.% Cu, respectively. Five ternary compounds and their solid solutions have been observed in this work: $CeAl_{12-x}Cu_x$ ($4.0 \le x \le 4.52$), $Ce_2Al_{17-x}Cu_x$ ($6.50 \le x \le 7.55$), $CeAl_{13-x}Cu_x$ ($6.62 \le x \le 6.92$), $CeAl_{4-x}Cu_x$ ($0.74 \le x \le 1.10$) and CeAlCu.
© 2009 Published by Elsevier B.V.

1. Introduction

Bulk metallic glasses (BMGs), as a new kind of materials, have attracted extensive interests and gained rapid development in the past decades. It is found that Ce-based amorphous metallic plastics (AMPs) exhibited extremely low glass transition temperature T_g down to about 68 °C, close to room temperature [1]. Ternary Ce–Al–Cu AMPs showed good glass forming ability (GFA) and could be easily fabricated in a wide composition range by conventional copper mold cast technique. The Ce-based AMP is a model material to investigate some basically important issues concerning the glass transition and supercooled metallic liquid. A study on phase relations of the ternary system Ce–Al–Cu can provide useful information for better understanding the formation and performance of the AMPs.

In Ref. [2], the phase diagram of binary Al–Ce system was assessed. There are five intermetallic compounds in the Al–Ce system, namely: Ce_3Al_{11}, $CeAl_3$, $CeAl_2$, CeAl and Ce_3Al. The phase diagram of Al–Cu system was reported in Ref. [3], and the existence of Al_2Cu and AlCu was confirmed. In the reported binary Ce–Cu system [4], the intermetallic compounds $CeCu_5$ and CeCu were confirmed. Existence of ternary compounds: $CeAl_{12-x}Cu_x$ ($4.0 \le x \le 4.55$), $CeAl_{4-x}Cu_x$ ($0.75 \le x \le 1$), $Ce_2Al_{17-x}Cu_x$ ($6.5 \le x \le 7.3$), $CeAl_{6.5}Cu_{6.5}$ and CeAlCu, was reported in Refs. [5–9]. However, there is no report about the phase relationships in the ternary Ce–Al–Cu system. In this work, we focus on the investigation of the phase relations in the ternary Ce–Al–Cu system in the Cu-poor part at 503 K.

2. Experimental

Two hundred and ten samples, each weighing 4 g, were prepared by arc melting high purity cerium, aluminum and copper metal blocks (purity > 99.8 wt.%) in an atmosphere of high purity argon. Then, the samples were turned and remelted eight times to ensure homogeneity. Each ingot was enclosed in evacuated quartz tubes and annealed for 5 months at 503 K. Finally, the samples were quenched into an ice-cold mixture. Considering that the Ce-based alloys oxidize quickly in the air, these samples were kept in the gasoline and every step of our experiment was carefully treated. Possible oxidized surface of the sample was removed before grinding the sample into powder for X-ray powder diffraction (XRD) experiments.

The powdered samples were investigated by XRD on a Rigaku D/Max-2500 diffractometer using Cu Kα radiation (45 kV × 250 mA) and a graphite monochromator for the diffracted beam in the range of $2\theta = 12 - 140°$. A continuous scanning mode with rate of $4°\ (2\theta)\ min^{-1}$ was used for routine phase identification, and a step scanning mode with a step width of $2\theta = 0.02°$ and a sampling time of 1 s was used for accurate determination of lattice parameters and crystal structure refinements. The structure and lattice parameters of the samples were refined by the Rietveld refinement program Fullprof.2k (Version 2.40).

3. Results and discussion

3.1. Phase analysis

In the Ce–Al–Cu ternary system (Cu-poor portion), nine binary compounds, namely Ce_3Al_{11}, $CeAl_3$, $CeAl_2$, CeAl, Ce_3Al,

* Corresponding author. Tel.: +86 773 5601517; fax: +86 773 5601517.
E-mail address: qingry96@guet.edu.cn (Q.R. Yao).

0925-8388/$ – see front matter © 2009 Published by Elsevier B.V.
doi:10.1016/j.jallcom.2009.03.126

Table 1
Crystallographic data of the compounds in the Ce–Al–Cu system (Cu-poor portion) at 503 K.

Phase	Space group	Pearson symbol and prototype	Lattice parameter (Å)			Ref.
			a	*b*	*c*	
β (α-Ce_3Al_{11})	*Immm*	*oI*28-αLa_3Al_{11}	4.3783(6)	12.9802(3)	10.0933(3)	This work
			4.3783(6)	13.02	10.09	[2]
γ($CeAl_3$)	$P6_3/mmc$	*hP*8-Ni_3Sn	6.5489(3)	–	4.6110(2)	This work
			6.547	–	4.61	[2]
δ($CeAl_2$)	$Fd\bar{3}m$	*cF*24-Cu_2Mg	8.0612(3)	–	–	This work
			8.061	–	–	[2]
ε(CeAl)	*Cmcm*	*oC*16-CeAl	9.269	7.680	5.761	[10]
ζ(α-Ce_3Al)	$P6_3/mmc$	*hP*8-Ni_3Sn	7.042	–	5.451	[10]
ι(CeCu)	*Pnma*	*oP*8-FeB	7.370	4.623	5.648	[11]
θ(Al_2Cu)	$I4/mcm$	*tI*12-Al_2Cu	6.0681(4)	–	4.8768(6)	This work
			6.067	–	4.877	[3]
η_2(AlCu)	$C2/m$	*mC*20-CuAl(r)	12.0606(3)	4.1047(2)	6.9123(6)	This work
			12.066	4.105	6.913	[3]
$^*\tau_1$($CeAl_8Cu_4$)	$I4/mmm$	*tI*26-$ThMn_{12}$	8.8223(2)	–	5.1557(3)	This work
			8.84	–	5.17	[5]
$^*\tau_4$($CeAl_3Cu$)	$I4/mmm$	*tI*10-$BaAl_4$	4.2633(4)	–	10.6852(6)	This work
			4.25	–	10.65	[6]
$^*\tau_2$($Ce_2Al_{10.2}$ $Cu_{6.8}$)	$R\bar{3}m$	*hR*57-Th_2Zn_{17}	8.9501(3)	–	13.0452(3)	This work
$^*\tau_2$(Ce_2Al_{10} Cu_7)			8.97	–	13.06	[7]
$^*\tau_3$($CeAl_{6.5}Cu_{6.5}$)	$Fm\bar{3}c$	*cF*112-$NaZn_{13}$	11.8754(1)	–	–	This work
			11.822	–	–	[8]
α($Ce(Al_{0.4}Cu_{0.6})_5$)	$P6/mmm$	*hP*6-$CaCu_5$	5.2573(2)	–	4.1824(1)	This work
			5.25	–	4.17	[15]
$^*\tau_5$(CeAlCu)	*p-62m*	*hP*9-Fe_2P	7.176	–	4.201	[9]

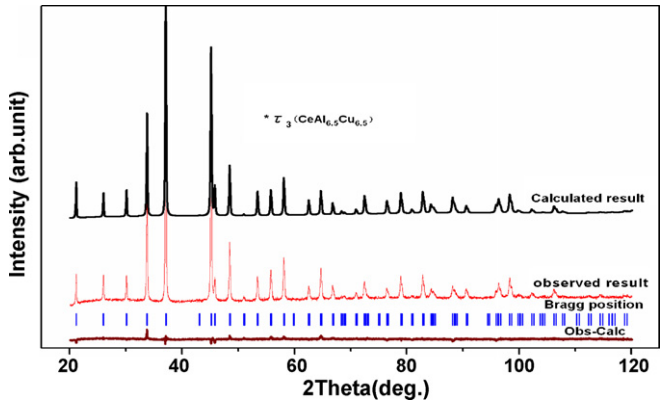

Fig. 1. The Rietveld refinement results of the XRD pattern of $^*\tau_3(CeAl_{6.5}Cu_{6.5})$ compound, including the calculated result, the observed result and difference intensities between them (lower line). The vertical bars indicate the expected Bragg reflection positions.

CeCu, $CeCu_5$, Al_2Cu, AlCu [2–4], and five ternary compounds: $CeAl_{12-x}Cu_x$ ($4.0 \le x \le 4.55$), $CeAl_{4-x}Cu_x$ ($0.75 \le x \le 1$), $Ce_2Al_{17-x}Cu_x$ ($6.5 \le x \le 7.3$), $CeAl_{6.5}Cu_{6.5}$ and CeAlCu [5–9] have been reported. The crystal structure data derived from our Rietveld refinements or reported in literature for the observed compounds are listed in Table 1. The refinement result of the XRD data of $^*\tau_3(CeAl_{6.5}Cu_{6.5})$ is shown in Fig. 1 as an example. The agreement between the observed and calculated profiles is excellent. The refinement results for $^*\tau_3(CeAl_{6.5}Cu_{6.5})$ are R_{wp} (%) = 14.3, R_p (%) = 12.2, R_{exp} (%) = 10.7, a = 11.8754(1) Å and V = 1674.73(4) Å^3.

In addition to the phases observed in our investigated samples and listed in Table 1, the compounds Al_3Cu_2 were reported in Ref. [12]. However, under our experimental conditions, the XRD analysis of the samples with the compositions close to "Al_3Cu_2" shows the coexistence of Al_2Cu and AlCu phases. Fig. 2 shows the XRD pattern of the "Al_3Cu_2" alloy.

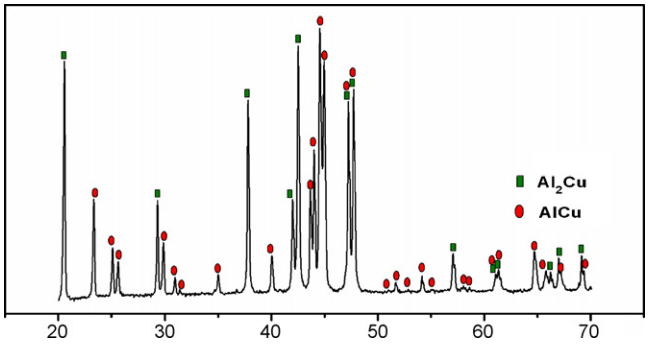

Fig. 2. XRD pattern of the sample Al_3Cu_2 indicates the two phases: Al_2Cu and AlCu.

3.2. Solid solubility limit

Refs. [5–9] reported composition ranges of some solid solution phases in the Ce–Al–Cu system. According to Refs. [13–14], the single-phase composition ranges of Al_2Cu and AlCu extend from

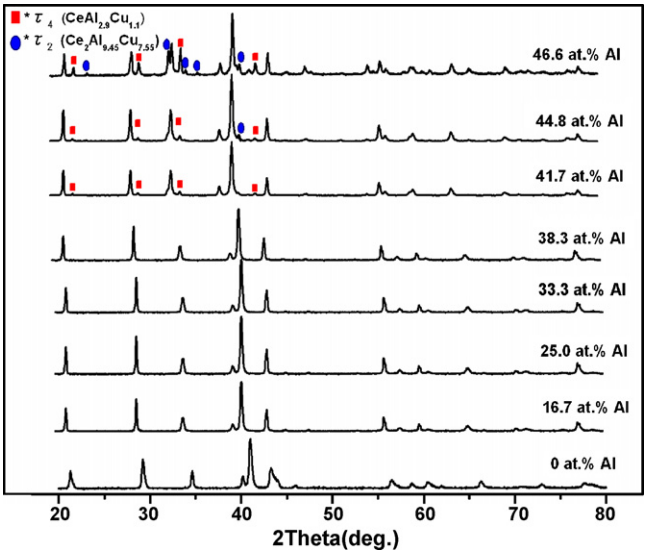

Fig. 3. XRD patterns of compound α($Ce_{0.167}Cu_{0.833-x}Al_x$) with different *x*.

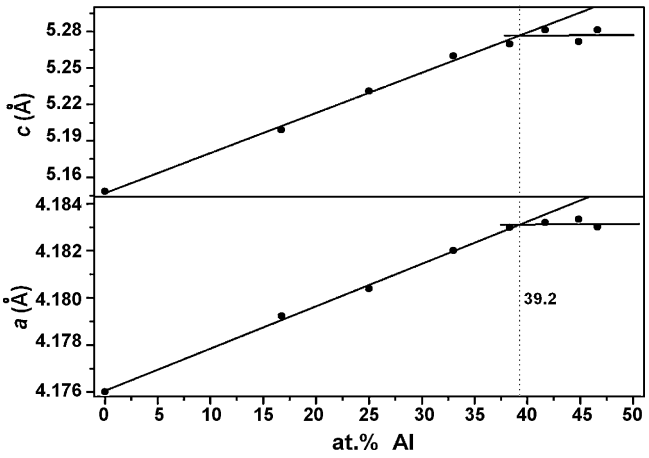

Fig. 4. The variation of lattice parameters of alloys $\alpha(Ce_{0.167}Cu_{0.833-x}Al_x)$ on Al content x.

32.05 to 32.6 at.% Cu and 49.8 to 52.3 at.% Cu, respectively. The solid solution of $CeCu_5$ is reported in Ref. [15]: $CeAl_{5-x}Cu_x$ ($0 \le x \le 2.10$). Based on the variation of the derived unit cell dimensions with the concentration of substituting component, we have determined that the maximum solid solubilitiy of Al in $CeCu_5$ is about 39.2 at.% Al, as shown in Figs. 3 and 4 . Fig. 3 shows XRD patterns of alloys with different Al content from 0 to 46.6 at.% in $\alpha(Ce_{0.167}Cu_{0.833-x}Al_x)$. The reflections from $^*\tau_4(CeAl_{2.9}Cu_{1.1})$ and $^*\tau_2(Ce_2Al_{9.45}Cu_{7.55})$ can be observed when the Al content exceeds 39.2 at.%. The variation of lattice parameters of alloys with Al contents in $\alpha(Ce_{0.167}Cu_{0.833-x}Al_x)$ is illustrated in Fig. 4. The lattice parameters a and c increase with increasing Al content. Likewise, the maximum solid solubilities of Cu in Al, α-Ce_3Al_{11}, $CeAl_3$ and $CeAl_2$ are determined to be about 2.5, 1.6, 3.6 and 5.3 at.%, respectively, and the homogeneity ranges of Al_2Cu and AlCu extend from about 32.1 to 32.6 at.% Cu and 49.7 to 52.4 at.% Cu, respectively. We have determined the solid solubilities of the four ternary compounds in this system: $CeAl_{12-x}Cu_x$ ($4.0 \le x \le 4.52$), $CeAl_{4-x}Cu_x$ ($0.74 \le x \le 1.10$), $Ce_2Al_{17-x}Cu_x$ ($6.50 \le x \le 7.55$) and $CeAl_{13-x}Cu_x$ ($6.62 \le x \le 6.92$). However, no apparent solid solubility was detected in CeAl, CeAlCu, α-Ce_3Al, CeCu and γ-Ce under our experimental conditions.

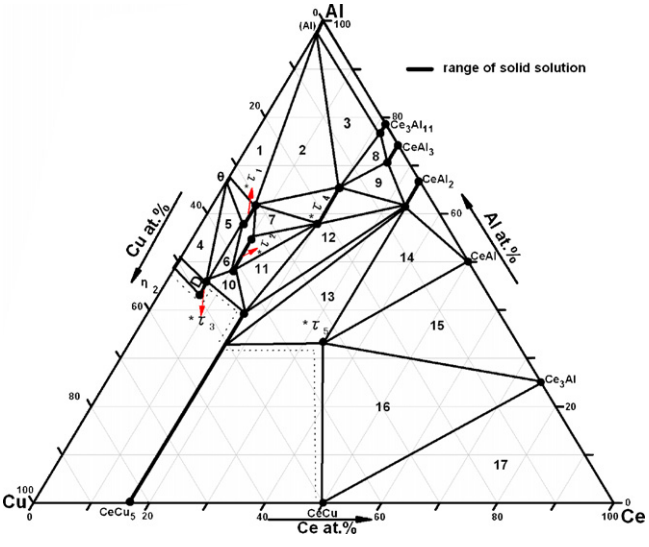

Fig. 5. The phase relations of the ternary Ce–Al–Cu system in the Cu-poor part at 503 K. The reported composition region of the bulk glass alloys in the Ce–Al–Cu system [1] falls in regions 15–17.

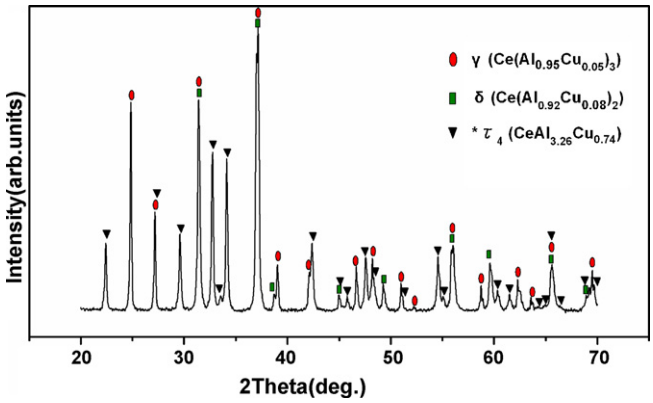

Fig. 6. XRD pattern of alloy $Ce_{27}Al_{66}Cu_7$ situated in the three-phase region 9.

3.3. Phase relationships

By comparing the X-ray diffraction patterns and identifying the phases in each sample, phase relationships of the Ce–Al–Cu ternary system were determined (shown in Fig. 5). The XRD pattern of the alloy $Ce_{27}Al_{66}Cu_7$, which falls in the region 9 and corresponds to three phases $^*\tau_4(CeAl_{3.26}Cu_{0.74}) + \gamma(Ce(Al_{0.95}Cu_{0.05})_3) + \delta(Ce(Al_{0.92}Cu_{0.08})_2)$, is illustrated in Fig. 6.

Phase regions 15, 16 and 17 are of particular interest. The reported composition region of the bulk glass alloys in the Ce–Al–Cu system [1] falls in this three phase regions. Among these BMGs, $Ce_{70}Al_{10}Cu_{20}$ exhibited the lowest glass transition temperature T_g of 341 K. The XRD patterns of the alloy MP001 obtained after annealing or by suck-cast into a copper mold are illustrated in Fig. 7. The annealed sample consists of three phases: γ-Ce + α-Ce_3Al + CeCu and falls in the region 17.

According to all the results obtained, the phase relations of the ternary system Ce–Al–Cu in the Cu-poor part at 503 K were determined, as shown in Fig. 5. The investigated composition region consists of 16 single-phase, 32 two-phase and 17 three-phase regions. The 16 single-phase regions are: $\theta(Al_2Cu)$, η_2(AlCu), $^*\tau_1(CeAl_{12-x}Cu_x)$, $^*\tau_2(Ce_2Al_{17-x}Cu_x)$, $^*\tau_3(CeAl_{13-x}Cu_x)$, $^*\tau_4(CeAl_{4-x}Cu_x)$, $^*\tau_5$(CeAlCu), $\alpha(CeCu_5)$, $\beta(\alpha\text{-}Ce_3Al_{11})$, $\gamma(CeAl_3)$, $\delta(CeAl_2)$, ε(CeAl), $\zeta(\alpha\text{-}Ce_3Al)$, ι(CeCu), κ(Al) and $\lambda(\gamma\text{-Ce})$. The 32 two-phase regions are: $\kappa+\theta$, $\kappa+{}^*\tau_1$, $\kappa+{}^*\tau_4$, $\kappa+\beta$, $\theta+{}^*\tau_1$, ${}^*\tau_1+{}^*\tau_2$, ${}^*\tau_2+{}^*\tau_4$, ${}^*\tau_1+{}^*\tau_4$, ${}^*\tau_4+\beta$, ${}^*\tau_4+\gamma$, $\beta+\gamma$, $\gamma+\delta$, ${}^*\tau_4+\delta$, $\alpha+\delta$, ${}^*\tau_4+\alpha$, $\alpha+{}^*\tau_2$, ${}^*\tau_3+\alpha$, ${}^*\tau_2+{}^*\tau_3$, ${}^*\tau_1+{}^*\tau_3$, $\theta+{}^*\tau_3$, $\eta_2+{}^*\tau_3$, $\theta+\eta_2$, $\alpha+{}^*\tau_5$, $\delta+{}^*\tau_5$, $\delta+\varepsilon$, $\varepsilon+{}^*\tau_5$, $\varepsilon+\zeta$, $\zeta+{}^*\tau_5$, $\iota+{}^*\tau_5$, $\zeta+\iota$, $\lambda+\zeta$, $\lambda+\iota$. The 17 three-phase regions are: $\kappa+\theta+{}^*\tau_1$, $\kappa+{}^*\tau_1+{}^*\tau_4$, $\kappa+{}^*\tau_4+\beta$, $\theta+\eta_2+{}^*\tau_3$, $\theta+{}^*\tau_3+{}^*\tau_1$, ${}^*\tau_3+{}^*\tau_1+{}^*\tau_2$, ${}^*\tau_1+{}^*\tau_2+{}^*\tau_4$, ${}^*\tau_4+\beta+\gamma$,

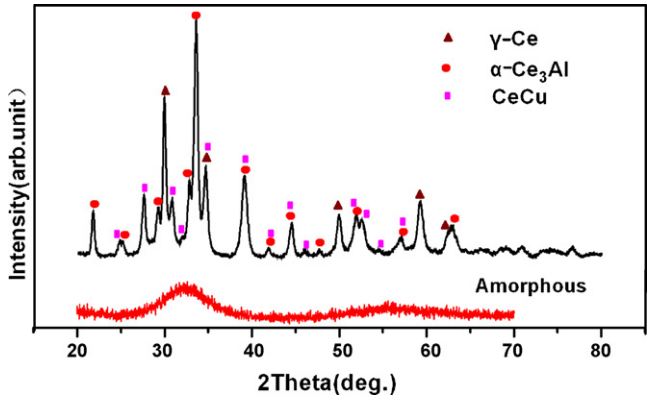

Fig. 7. XRD patterns of alloy $Ce_{70}Al_{10}Cu_{20}$ obtained after annealing (top) or by suck-cast into a copper mold (bottom).

Table 2
Identification of phase for the ternary alloy in each three-phase region in the Ce–Al–Cu ternary system in the Cu-poor part at 503 K.

Phase regions	XRD identified phases	Ternary alloys
1	$\kappa+\theta+{}^*\tau_1$	$Ce_3Al_{72}Cu_{25}$
2	$\kappa+{}^*\tau_1+{}^*\tau_4$	$Ce_{10}Al_{70}Cu_{20}$
3	$\kappa+{}^*\tau_4+\beta$	$Ce_{15}Al_{79}Cu_6$
4	$\theta+\eta_2+{}^*\tau_3$	$Ce_3Al_{52}Cu_{45}$
5	$\theta+{}^*\tau_3+{}^*\tau_1$	$Ce_{4.6}Al_{60}Cu_{35.4}$
6	${}^*\tau_3+{}^*\tau_1+{}^*\tau_2$	$Ce_8Al_{51}Cu_{41}$
7	${}^*\tau_1+{}^*\tau_2+{}^*\tau_4$	$Ce_{12}Al_{58}Cu_{30}$
8	${}^*\tau_4+\beta+\gamma$	$Ce_{23}Al_{72}Cu_5$
9	${}^*\tau_4+\gamma+\delta$	$Ce_{26}Al_{67}Cu_7$
10	${}^*\tau_3+{}^*\tau_2+\alpha$	$Ce_{11}Al_{45}Cu_{44}$
11	${}^*\tau_2+\alpha+{}^*\tau_4$	$Ce_{15}Al_{49}Cu_{36}$
12	$\alpha+{}^*\tau_4+\delta$	$Ce_{24}Al_{56}Cu_{20}$
13	$\delta+\alpha+{}^*\tau_5$	$Ce_{31}Al_{45}Cu_{24}$
14	${}^*\tau_5+\varepsilon+\delta$	$Ce_{40}Al_{50}Cu_{10}$
15	${}^*\tau_5+\varepsilon+\zeta$	$Ce_{60}Al_{35}Cu_{15}$
16	${}^*\tau_5+\zeta+\iota$	$Ce_{65}Al_{25}Cu_{15}$
17	$\zeta+\iota+\lambda$	$Ce_{70}Al_{10}Cu_{20}$

${}^*\tau_4+\gamma+\delta$, ${}^*\tau_3+{}^*\tau_2+\alpha$, ${}^*\tau_2+\alpha+{}^*\tau_4$, $\alpha+{}^*\tau_4+\delta$, $\delta+\alpha+{}^*\tau_5$, ${}^*\tau_5+\varepsilon+\delta$, ${}^*\tau_5+\varepsilon+\zeta$, ${}^*\tau_5+\zeta+\iota$, $\zeta+\iota+\lambda$. The constitutions of the three-phase regions and one representative sample in each three-phase region we prepared are listed in Table 2.

4. Conclusions

(1) Based on XRD phase identification, the phase relations of the ternary system Ce–Al–Cu in the Cu-poor part at 503 K have been determined.
(2) Under our experimental conditions, the existence of the compounds: $\theta(Al_2Cu)$, $\eta_2(AlCu)$, ${}^*\tau_1(CeAl_{12-x}Cu_x)$, ${}^*\tau_2(Ce_2Al_{17-x}Cu_x)$, ${}^*\tau_3(CeAl_{13-x}Cu_x)$, ${}^*\tau_4(CeAl_{4-x}Cu_x)$, ${}^*\tau_5(CeAlCu)$, $\alpha(CeCu_5)$, $\beta(\alpha\text{-}Ce_3Al_{11})$, $\gamma(CeAl_3)$, $\delta(CeAl_2)$, $\varepsilon(CeAl)$, $\zeta(\alpha\text{-}Ce_3Al)$ and $\iota(CeCu)$, in the Ce–Al–Cu ternary system (Cu-poor portion) are confirmed and their solid solubilities are determined.
(3) The reported composition region of the bulk glass alloys in the Ce–Al–Cu system falls in regions 15–17. XRD shows that the alloy of MP001, which could be easily fabricated by copper mold cast technique as a metallic glass with T_g = 341 K, lies in phase region 17 consisting of three phases Ce, Ce_3Al and CeCu.

Acknowledgements

The experimental assistance and discussion with J. Luo, J.R. Chen, L.N. Ji and J. Yu are appreciated. The authors are grateful for the financial support of the Natural Science Foundation of China (Grant Nos. 50631040 and 50861006).

References

[1] B. Zhang, D.Q. Zhao, M.X. Pan, R.J. Wang, W.H. Wang, Acta Mater. 54 (2006) 3025–3032.
[2] M.C. Gao, N. Unlu, G.J. Shiflet, M. Mihalkovic, M. Widom, Metall. Mater. Trans. A 36 (2005) 3269–3279.
[3] X.J. Liu, I. Ohnuma, R. Kainuma, K. Ishida, J. Alloys Compd. 264 (1998) 201–208.
[4] P. Villars, Pearson's Handbook of Crystallographic Data for Intermetallic Phases, vols. 1–2, ASM International, Materials Park. OH, 1997.
[5] O.S. Zarechnyuk, P.I. Kripyakevich, Sov. Phys. Crystallogr. 7 (1963) 436–446.
[6] O.S. Zarechnyuk, P.I. Kripyakevich, E.I. Gladyshevskij, Sov. Phys. Crystallogr. 9 (1965) 706–708 (translated from Kristallografiya 9 (1964) 835–838).
[7] G. Cordier, E. Czech, H. Schäfer, J. Less-Common Met. 108 (1985) 225–239.
[8] G. Cordier, E. Czech, H. Schäfer, P. Woll, J. Less-Common Met. 110 (1985) 327–330.
[9] H. Oesterreicher, J. Less-Common Met. 30 (1973) 225–236.
[10] K.A. Gschneidner Jr., F.W. Calderwood, Bull. Alloy Phase Diagrams 9 (1988) 669–672.
[11] P.R. Subramanian, D.E. Laughlin, ASM Int. 10 (1994) 127–133.
[12] P. Ramachandrarao, M. Laridjani, J. Mater. Sci. 9 (1974) 434–437.
[13] T. Goedecke, F. Sommer, Z. Metallkd. 87 (7) (1996) 581–586.
[14] J.L. Murray, Int. Met. Rev. 30 (5) (1985) 211–233.
[15] T. Takeshita, S.K. Malik, W.E. Wallace, J. Solid State Chem. 23 (1978) 225–229.